

Assimilation of sialic crustal material by volcanics of the easternmost extension of the Trans-Mexican Volcanic Belt- Evidence from Sr and Nd isotopes

Thomas Besch¹, Surendra P. Verma², Ulrich Kramm³, Jörg F.W. Negendank⁴, Heiner J. Tobschall⁵ and Rolf Emmermann⁶

¹ Lehreinheit Mineralogie, Institut für Geowissenschaften, Universität Mainz, Germany.

² Max-Planck-Institut für Chemie, Abt. Geochemie, and Universität Trier, Abt. Geologie, Present address: Laboratorio de Energía Solar, Instituto de Investigaciones en Materiales, UNAM, Temixco, Mor., Mexico.

³ Universität Münster, Institut für Mineralogie, Münster, Germany.

⁴ Geoforschungszentrum Potsdam and Geowissenschaften, Universität Potsdam, Potsdam, Germany.

⁵ Institut für Geologie und Mineralogie, Universität Erlangen-Nürnberg, Erlangen, Germany.

⁶ Geoforschungszentrum Potsdam, Potsdam FRG, and Institut für Geowissenschaften und Lithosphärenforschung, Universität Gießen, Gießen, Germany.

Received: April 30, 1993; accepted: June 16, 1994.

RESUMEN

Las rocas volcánicas basálticas hasta riolíticas, de edad Plioceno al Cuaternario, provenientes de la parte extrema oriental de la Faja Volcánica Trans-Mexicana (FVTM), se caracterizan por $^{87}\text{Sr}/^{86}\text{Sr}$ de 0.70342 a 0.70511 y $^{143}\text{Nd}/^{144}\text{Nd}$ de 0.51250 a 0.51287. Dado que las rocas volcánicas son muy jóvenes (de edad Plioceno al Cuaternario), se pueden considerar estas relaciones isotópicas medidas como las iniciales. Estos isótopos se correlacionan negativamente y, con una excepción, caen en el campo del 'arreglo del manto'. La variación isotópica no se puede explicar por modelos binarios sencillos, ni por modelos de tipo AFC. Nuestra interpretación sugiere un modelo complejo involucrando las heterogeneidades en el manto y la asimilación del material cortical.

PALABRAS CLAVE: Rocas volcánicas, Plioceno, Cuaternario, FVTM, estroncio, neodimio, manto, corteza, asimilación.

ABSTRACT

Pliocene to Quaternary basaltic to rhyolitic volcanics of the easternmost part of the TMVB are characterized by $^{87}\text{Sr}/^{86}\text{Sr}$ ratios from 0.70342 to 0.70511 and $^{143}\text{Nd}/^{144}\text{Nd}$ ratios from 0.51250 to 0.51287. Since the volcanics are of Pliocene to Quaternary age, the measured Sr and Nd isotope ratios are taken as initial ratios. These isotope ratios are negatively correlated and, with one exception, plot on the 'mantle array'. The isotopic variation cannot be explained by simple binary mixing models or AFC-modelling. Our interpretation suggests a complex model involving mantle heterogeneities and assimilation of crustal material.

KEY WORDS: Volcanic rocks, Pliocene, Quaternary, TMVB, strontium, neodium, mantle, crust, assimilation.

INTRODUCTION

The Trans-Mexican Volcanic Belt (TMVB) is a roughly west-east trending structure presumably formed in association with the subduction of the Cocos/Rivera plate system (Robin, 1976, 1982; Demant, 1978, 1981; Pal *et al.*, 1978; Nixon, 1982; Verma, 1985, 1987a, b; Negendank *et al.*, 1985; Besch *et al.*, 1987; Nixon *et al.*, 1987; Verma and Nelson, 1989a, b). Our study area (Figure 1) lies in the easternmost extension of the TMVB, where according to several authors two different volcanic provinces, the calc-alkaline association of the W-E trending TMVB and a N-S orientated alkaline province, overlap (Robin, 1976; Demant, 1978; Thorpe, 1977; Pichler and Weyl, 1976). We present here our $^{87}\text{Sr}/^{86}\text{Sr}$ and $^{143}\text{Nd}/^{144}\text{Nd}$ isotope data on selected samples from the easternmost part of the TMVB and discuss their petrogenetic implications.

GEOLOGY AND GEOCHEMISTRY

According to Negendank *et al.* (1985) the eastern TMVB can be divided into four geological units, which are

from W to E: the Altiplano Area (Oriental Basin) (approximately left half area, left of Pico de Orizaba, in Figure 2), the Cofre de Perote - Pico de Orizaba Range (right half area in Figure 2), the Jalapa-Naolinco Area (left half area in Figure 3), and the Palma Sola Massif (right half area in Figure 3). During the Pliocene to Quaternary, several stratovolcanoes, domes, lava flows, monogenetic cones and maars were formed erupting rocks belonging to the calc-alkaline, high-K and shoshonitic series. On the basis of microprobe mineral analysis of recent lavas from volcán Pico de Orizaba, Kudo *et al.* (1985) concluded that xenolithic contamination was an important petrogenetic process during their evolution.

Besch *et al.* (1988) have reported the major, trace and rare-earth element characteristics of 30 samples. In the present paper additionally the results of $^{87}\text{Sr}/^{86}\text{Sr}$ and $^{143}\text{Nd}/^{144}\text{Nd}$ isotope ratios are presented. The investigated rocks are located in the easternmost extension of the TMVB (locations are given in Figures 2 and 3) and have been selected from different geological units to examine the sug-

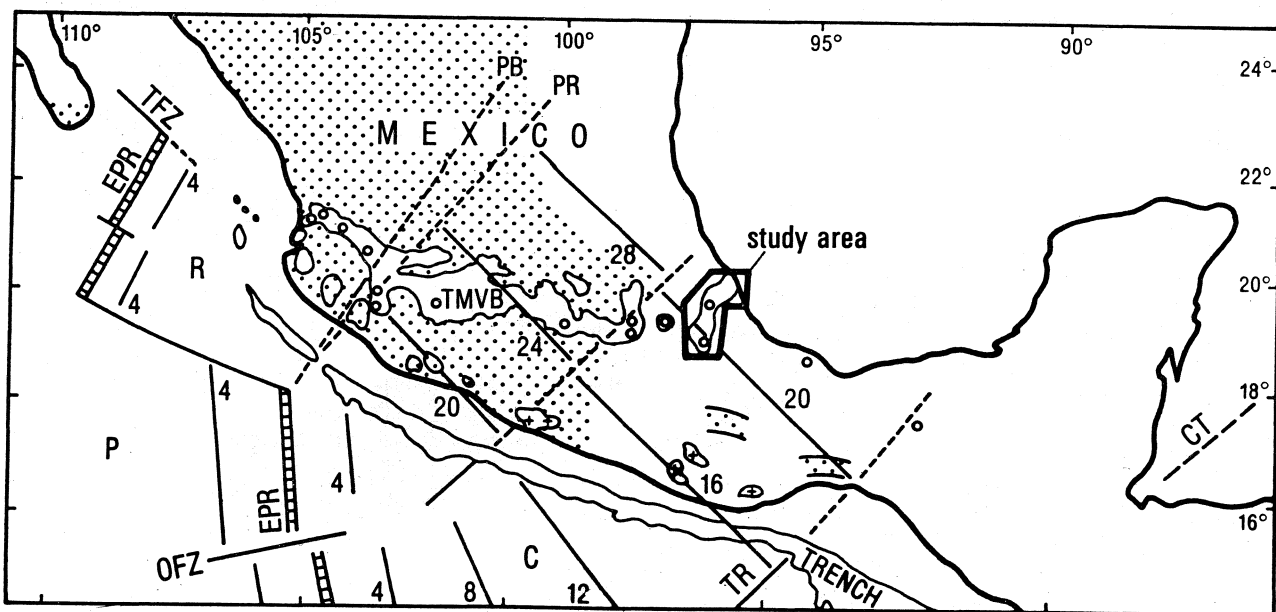


Fig. 1. A simplified map showing the study area in context of the TMVB. C = Cocos plate, CT = Cayman trough, EPR = East Pacific Rise, P = Pacific plate, R = Rivera plate, PB = transform boundary between Rivera and Cocos plates (predicted), PR = trend of proto-Rivera fracture zone if one was indeed present in the subducted plate, TMVB = Trans-Mexican Volcanic Belt, TFZ = Tamayo fracture zone, TR = Tehuantepec ridge.

gested comagmatic relationships for all rock types. The volcanic rocks are classified as alkali basalt, transitional basalt, basaltic andesite, andesite, dacite and rhyolite. The foid-free basalts without normative nepheline were considered by Negendank *et al.* (1985) as transitional basalts. Additionally, the andesites are divided into basaltic, monogenetic and stratovolcano andesites.

The Altiplano Area (Oriental Basin)

The central part of the Altiplano is dominated by the rhyolite domes of Cerro Derrumbadas and Cerro Pinto (Figure 2). These are surrounded by several monogenetic cones of andesitic, dacitic and, in minor amounts, transitional basaltic compositions. Rare-earth element patterns for the volcanic rocks are shown in Figure 4. All andesite types and dacites are LREE- (light rare-earth element) enriched with Ce/Yb_n -ratios clustered varying around 6.3 and have flat HREE (heavy rare-earth element) distribution. In the Oriental Basin there is no tendency for the absolute REE (rare-earth element) abundances to increase with the degree of fractionation, precluding a cogenetic relationship for the volcanics.

The REE patterns for the Cerro Derrumbadas rhyolites (Figure 4) exhibit LREE-enrichment ($\text{Ce}/\text{Yb}_n = 111$), depleted HREE and a slight negative Europium anomaly. According to Besch *et al.* (1988) these patterns cannot be derived by fractionation processes involving a basaltic parental magma. The Cerro Derrumbadas rhyolite (sample NT5, Figures 2 and 4) might represent a partial melt of the continental crust involving residual garnet, amphibole and plagioclase. The Cerro Pinto rhyolite (sample NH33, Fi-

gures 2 and 4) exhibits a flat LREE ($\text{Ce}/\text{Yb}_n = 1.4$) and a flat HREE distribution and has a distinct negative Europium anomaly. Even the Cerro Pinto rhyolite might represent a partial melt of the continental crust, but in contrast to the Cerro Derrumbadas rhyolite with residual orthopyroxene, clinopyroxene and plagioclase. Multi-element normalized plots (Figure 4) for the volcanics, excluding the rhyolites, reveal distinct negative anomalies of Nb, Ta, Ti, and high LILE/HFSE (large ion lithophile (LILE) vs. high field strength elements (HFSE)) ratios suggesting a subduction related petrogenesis.

Cofre de Perote - Pico de Orizaba Range

This area (Figure 2) is characterized by the stratovolcanoes Cofre de Perote and Pico de Orizaba. These volcanoes are built mostly of andesite and dacite lava flows. Additionally, several monogenetic cinder cones of erupted transitional basalts ('hawaiites' according to Negendank *et al.*, 1985) and basaltic andesites occur in that area. Rare-earth element patterns for the volcanic rocks are presented in Figure 4. All rock types are LREE-enriched with Ce/Yb_n -ratios varying around 5.2. Europium anomalies are absent. There is no tendency for the absolute REE abundances to increase with the degree of fractionation. This precludes a cogenetic relationship between the basalts and andesites in this area.

Multi-element normalized diagrams (Figure 4) for the Cofre de Perote and Pico de Orizaba volcanics, normalized by using primitive mantle values by Jagoutz *et al.* (1979) and Wänke *et al.* (1984), display a high ratio of LILE/HFSE and distinct negative anomalies of Ta, Nb and Ti for

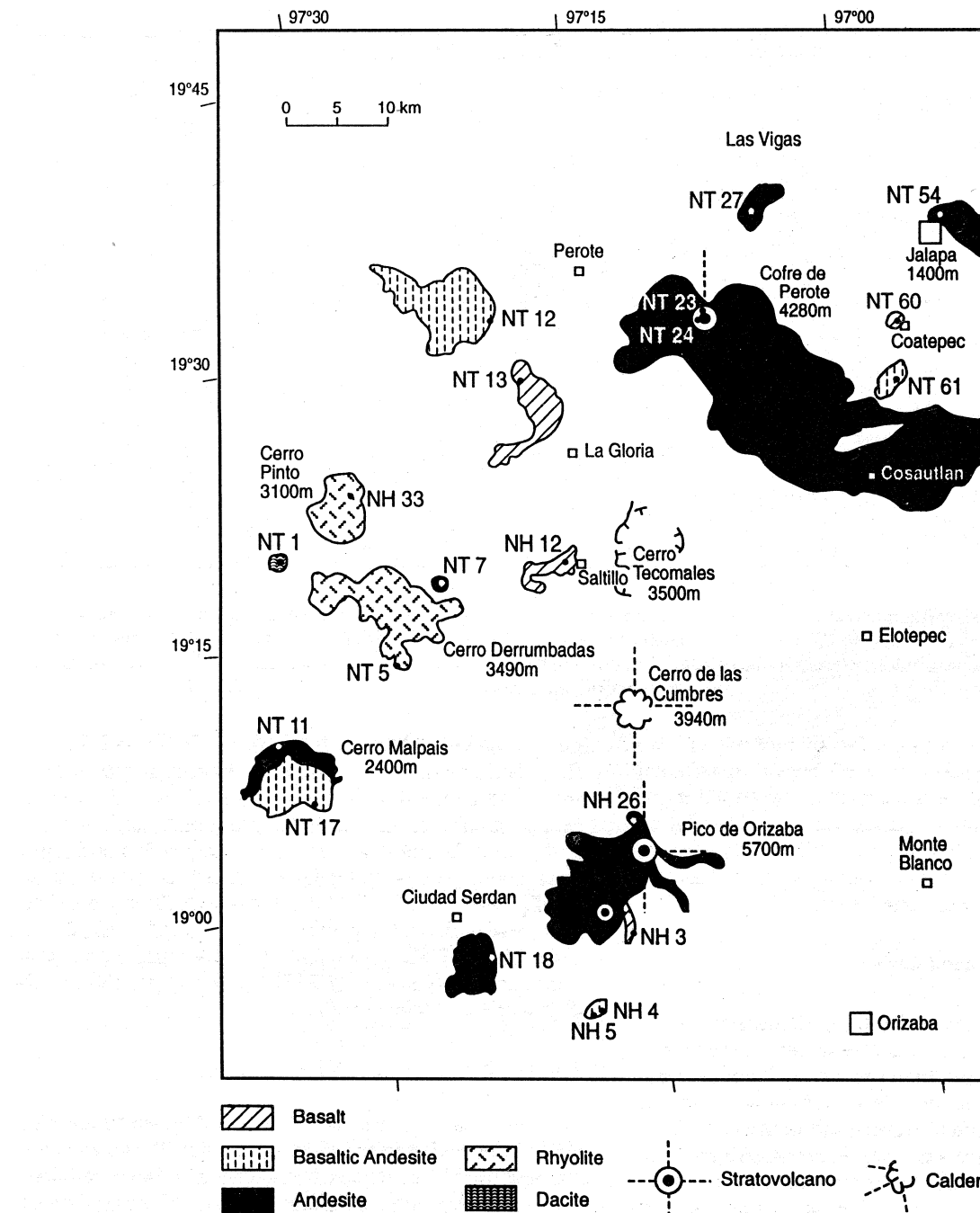


Fig. 2. Simplified geological map of the Altiplano Area (Altiplano/Pico de Orizaba-Cofre de Perote Range), modified according to Negendank *et al.* (1985).

the stratovolcano andesites. These geochemical signatures are indicative of subduction related volcanics (Pearce, 1982; Brihuega *et al.*, 1984). The Morb normalized trace element patterns (Besch *et al.*, 1988) of the primitive basalts in this area (Figure 4), show a clear enrichment in LILE relative to MORB, suggesting a LILE-enriched source for the Cofre de Perote-Pico de Orizaba basalts.

Jalapa-Naolinco Area

The Jalapa-Naolinco Area (Figure 3) is dominated by cinder cones that erupted alkali basalts, transitional basalts

and calc-alkaline andesites. REE patterns for the volcanics are shown in Figure 4. All rock-types are LREE-enriched with Ce/Yb_n-ratios varying from 4.5 (basalts) to 9.1 (alkali basalts) and exhibit flat HREE distribution. Europium anomalies are absent.

Multi-element normalized diagrams (Figure 4) show that the basalts and basaltic andesites have lower incompatible trace element concentrations than the alkaline rocks. Since fractionation would increase the concentration of incompatible elements, the derivation of calc-alkaline rocks from the alkaline rocks is excluded.

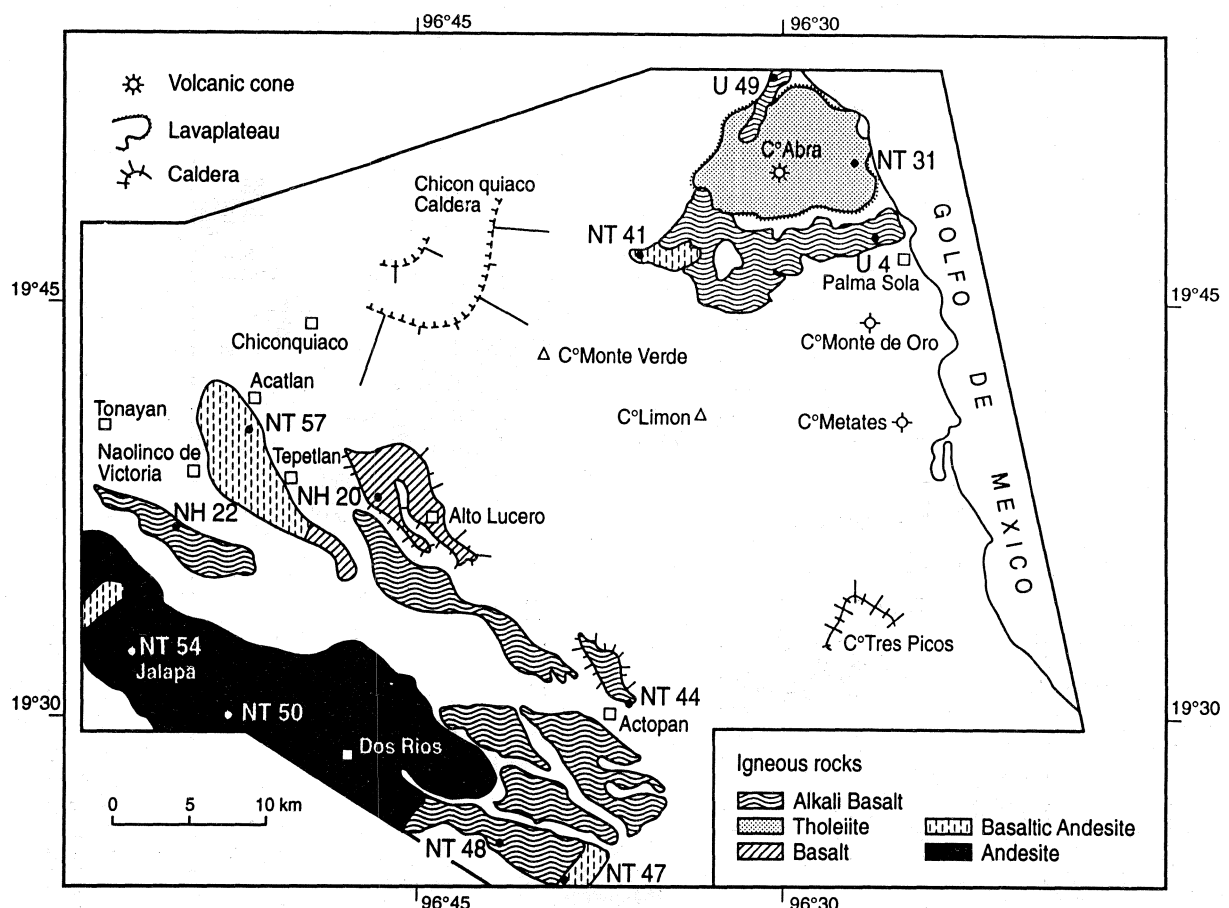


Fig. 3. Simplified geological map of the Jalapa - Chiconquiaco - Palma Sola Area, modified according to Negendank *et al.* (1985).

Additionally, according to Besch *et al.* (1988) all rock types are characterized by high LILE/HFSE ratios and distinct negative anomalies of Nb, Ta and Ti, even for the alkali basalts. This geochemical signature implies a subduction relationship for the volcanics or an involvement of a subduction-modified mantle source region. Typical intraplate volcanics induced by crustal rifting have a Ta, Nb and Ti spike (Wood, 1979). Multi-element diagrams (Figure 4) for primitive basalts and alkali basalts, normalized to average MORB, indicate that the mantle source for the volcanics was LILE-enriched.

Palma Sola Massif

The volcanism in the Palma Sola Massif (Figure 3) is dominated by alkaline volcanics with subordinate calc-alkaline andesites and dacites. REE patterns (Figure 4) indicate LREE-enrichment in all volcanics with Ce/Yb_n-ratios varying from 5.8 (basalt) to 9.3 (basaltic andesite) and a flat HREE distribution. Europium anomalies are absent. There is no tendency for the REE concentrations to increase with the degree of fractionation, precluding a cogenetic relationship.

Multi-element diagrams (Figure 4), normalized by using primitive mantle values show distinct negative anomalies

of Nb, Ta and Ti as well as high LILE/HFSE ratios suggesting a subduction relationship. MORB normalized multi-element diagrams (Figure 4) reveal LILE-enrichment for the primitive basalts indicating a LILE-enriched mantle source.

Major element abundances of volcanic rocks from the eastern Trans Mexican Volcanic Belt indicate that the alkaline rocks and basalts were generated by crystal/liquid fractionation processes (Negendank *et al.*, 1985), whereas the andesites, dacites and rhyolites cannot be considered as final products of the same fractionation series.

The trace element patterns of the most primitive basalts were originated by partial melting of spinel-lherzolite (due to the unfractuated HREE) in the mantle wedge overlying the subduction zone whose incompatible element composition was modified by fluids and possibly sediments released from the subduction slab of the Cocos/Rivera plate association. This can even be related to an earlier plate association, e.g. a Paleopacific plate system. These fluids are richer in LILE than in Ta, Nb, Ti and other HFSE (Hole *et al.*, 1984). Another feature suggesting the derivation of magma from the mantle wedge is the depletion of Rb relative to Ba and Sr, as seen in the multi-element normalized

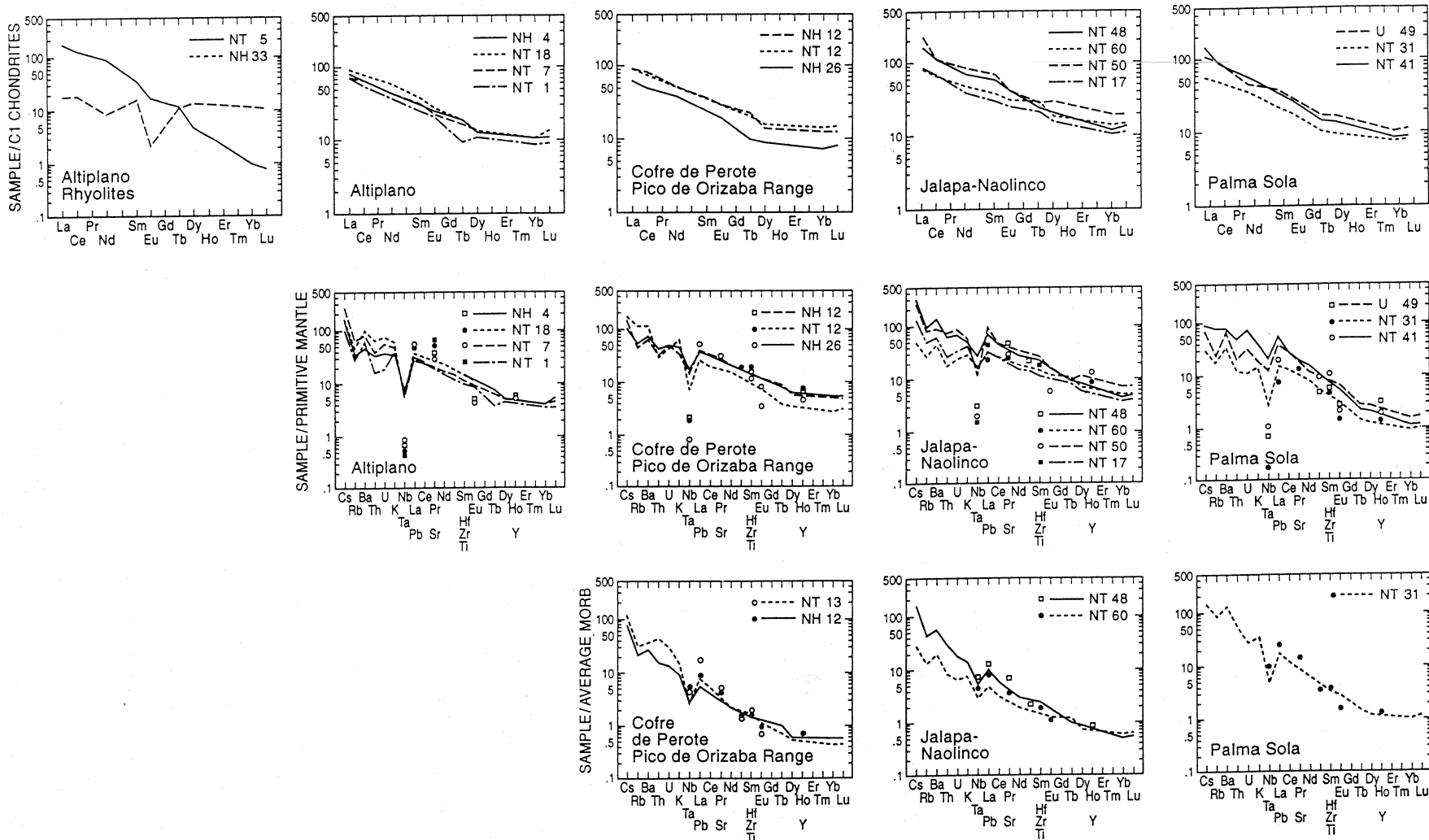


Fig. 4. Multi-element normalized diagrams of REE and trace elements of volcanics of the four geological units: Altiplano Area (Oriental Basin) (Fig. 2), Cofre de Perote - Pico de Orizaba Range (Fig. 2), Jalapa-Naolinco de Victoria Area (Fig. 3), Palma Sola Area (Fig. 3). These plots are modified according to Besch *et al.* (1988). For sample locations, names and concentration data, see Figs. 2 and 3, and Tables 1, 2 and 3.

diagrams, due to the greater incompatibility of Rb to fluids extracted from the downgoing slab (Ellam and Hawkesworth, 1987). This seems to be evident for the alkali basalts because they exhibit geochemical signatures much more similar to arc than intraplate volcanics.

The rhyolites in the eastern TMVB were interpreted as partial melts of the continental crust by Besch *et al.* (1988).

$^{87}\text{Sr}/^{86}\text{Sr}$ AND $^{143}\text{Nd}/^{144}\text{Nd}$ ISOTOPE RATIOS

The $^{87}\text{Sr}/^{86}\text{Sr}$ ratios of 30 selected samples (25 new and 5 published previously - Tobschall *et al.*, 1984) and $^{143}\text{Nd}/^{144}\text{Nd}$ ratios of 15 of these samples (10 new and 5 published previously - Tobschall *et al.*, 1984) from the easternmost extension of the TMVB have been determined using the following procedures.

Sr isotope compositions were measured on a 12", 90° sector, NBS design solid source mass spectrometer with on-line data reduction at the Zentraleinstitut für Geochronologie, Münster. Nd isotope compositions were measured on a Finnigan MAT 261 mass spectrometer at the Max-Planck-Institut für Chemie, Mainz. The procedures used for the Sr isotope determination are given in Kramm *et al.* (1983), those for the Nd-isotopes in White and Patchett (1984), with the difference that a triple collector (in peak-jumping mode) was employed for Nd. Total procedural blanks (1.5 ng Sr and 34 pg Nd) were negligible for this study. The results of these measurements are given in Table 1. All samples are geologically very young (0.01 - 5 Ma) and hence the $^{87}\text{Sr}/^{86}\text{Sr}$ and $^{143}\text{Nd}/^{144}\text{Nd}$ ratios reported in Table 1 are taken as initial ratios. Table 2 gives the major, trace and REE element abundances of these samples.

The $^{87}\text{Sr}/^{86}\text{Sr}$ ratios for the alkali basalts, basalts, basaltic andesites, andesites and rhyolites of the easternmost extension of the TMVB range from 0.70342 to 0.70511 and are comparable with similar rocks from other areas of the TMVB (Moorbath *et al.*, 1978; Whitford and Bloomfield, 1976; Cantagrel and Robin, 1978; Verma, 1983, 1984, 1994; Verma and Armienta-H., 1985; Verma *et al.*, 1985; Verma and Verma, 1986; McBirney *et al.*, 1987; Mahood and Halliday, 1988; Verma *et al.*, 1991; Verma and Luhr, 1993). For all rock types from the easternmost extension of the TMVB, a discrete range in the $^{87}\text{Sr}/^{86}\text{Sr}$ ratios (Table 3) is found.

Our results show that $^{87}\text{Sr}/^{86}\text{Sr}$ ($n = 27$) is positively correlated with the concentration of SiO_2 ($r = 0.808$), Rb ($r = 0.535$), K_2O ($r = 0.557$) and negatively with Sr ($r = -0.672$). Even after excluding the rhyolites, which possibly have a larger crustal component, basalts and andesites are characterized by a significant positive correlation of $^{87}\text{Sr}/^{86}\text{Sr}$ and SiO_2 ($r = 0.726$, $n = 25$). The correlation of

the $^{87}\text{Sr}/^{86}\text{Sr}$ ratios with SiO_2 (Figure 5) implies that the stratovolcano andesites acquired a crustal component during ascent. This conclusion is also compatible with the combined $^{143}\text{Nd}/^{144}\text{Nd}$ and $^{87}\text{Sr}/^{86}\text{Sr}$ data. The $^{143}\text{Nd}/^{144}\text{Nd}$ ratios for the analyzed samples from the easternmost extension of the TMVB range from 0.51250 to 0.51287. There is a significant negative correlation (Figure 6, $r = -0.858$, $n = 15$) between the initial $^{143}\text{Nd}/^{144}\text{Nd}$ and $^{87}\text{Sr}/^{86}\text{Sr}$ ratios for the analyzed samples. The data define a trend parallel to that of the 'mantle array', and thus no clear influence of interaction with seawater or subducted oceanic crust plus sediments (both processes should result in a shift towards the right of the 'mantle array' (Hawkesworth *et al.*, 1977 and White and Hofmann, 1982) seems to be visible. This, however, holds only if a distinctly different isotope signature is added. In the case of volcanogenic sediments derived from volcanic rocks at a 'young' continental margin, which can be assumed for southern Mexico, this method probably cannot discriminate the addition.

It can be seen from Figure 5 that the Sr isotopic compositions for the different rock types of the easternmost TMVB shows distinct range at fairly constant SiO_2 values. In other words, there is a 'vertical' variation of $^{87}\text{Sr}/^{86}\text{Sr}$ against SiO_2 superimposed on the overall positive correlation mentioned earlier. Furthermore, there is no correlation between the Mg-values and the $^{87}\text{Sr}/^{86}\text{Sr}$ ratios for each specific rock type. These results argue against simple AFC-modelling (DePaolo, 1981) to explain the isotopic variations. Even for the most primitive samples (Mg-values ~ 68) some scatter in the $^{87}\text{Sr}/^{86}\text{Sr}$ ratios is observable suggesting mantle heterogeneities. We tested several end-member possibilities (depleted as well as enriched mantle, based on the trace element data, several crustal model compositions and DSDP sites 487/488 sediments (S.P. VERMA, unpublished data) in simple binary mixing models in which the degree of curvature of predicted hyperbolic curves depends on the ratio of Sr/Nd in the selected end-members (DePaolo and Wasserburg, 1979).

The results of our calculations (Figure 7) are compatible with assimilation of upper crustal material during the uprise and magmatic evolution of the rock types. It should, however, be kept in mind that we do not have information about the composition of the lower crust beneath the easternmost TMVB. Our calculations show that the possibility of sedimentary input cannot be eliminated. The volcanic rocks in the easternmost TMVB are underlain by sedimentary rocks and so we cannot clearly discriminate the source of the sedimentary input, whether the subducted sediments or the underlying sedimentary rocks.

CONCLUSIONS

These isotopic data stimulate an intricate petrogenetic model that should include: (i) different heterogeneous mantle reservoirs, (ii) assimilation of continental crust, and probably (iii) recycling of subducted sediments.

Table 1

Isotope and trace element data for the volcanics of the easternmost TMVB

Sample ⁺	Rock type*	SiO ₂	Rb ^{**}	Sr ^{**}	⁸⁷ Sr/ ⁸⁶ Sr ^{*+*}	¹⁴³ Nd/ ¹⁴⁴ Nd ^{***}
NT 44	alkali basalt	43.5	27	1111	0.70361 ± 8	
U 4	alkali basalt	46.7	26	953	0.70364 ± 9	
U 49	alkali basalt	47.9	30	838	0.70342 ± 9	0.512866 ± 13
NT 48	alkali basalt	48.7	50	858	0.70394 ± 4	0.512842 ± 16
NT 31	tholeiite	52.2	21	593	0.70424	0.512683
NH 22	basalt	49.6	14	385	0.70346 ± 8	
NT 60	basalt	49.8	14	464	0.70414 ± 4	0.512753 ± 19
NH 12	basalt	50.6	21	511	0.70385 ± 7	0.512790 ± 17
NH 20	basalt	52.2	96	931	0.70408 ± 5	
NH 3	basalt	52.4	18	548	0.70439 ± 3	
NT 13	basalt	52.8	35	619	0.70393 ± 6	
NT 57	basaltic andesite	52.7	16	598	0.70425 ± 8	
NT 41	basaltic andesite	52.8	69	868	0.70371 ± 7	0.512816 ± 14
NH 4	basaltic andesite	53.3	18	701	0.70374 ± 6	0.512621 ± 28
NT 17	basaltic andesite	53.4	27	525	0.70424 ± 6	
NT 12	basaltic andesite	53.4	29	503	0.70415 ± 8	0.512771 ± 21
NH 5	basaltic andesite	53.7	17	691	0.70392 ± 9	
NT 61	monogenetic basaltic andesite	53.9	32	570	0.70405 ± 5	
NT 47	monogenetic andesite	54.4	100	406	0.70429 ± 8	
NT 54	monogenetic andesite	56.3	34	497	0.70443	0.512690
NT 18	monogenetic andesite	56.9	25	899	0.70374 ± 6	

Table 1 (Cont.)

Sample ⁺	Rock type*	SiO ₂	Rb ^{**}	Sr ^{**}	⁸⁷ Sr/ ⁸⁶ Sr ^{++*}	¹⁴³ Nd/ ¹⁴⁴ Nd ^{***}
NT 50	monogenetic andesite	57.1	45	540	0.70434 ± 7	
NT 11	monogenetic andesite	57.2	39	484	0.70456	0.512613
NT 27	monogenetic andesite	58.1	73	528	0.70430 ± 6	
NT 7	stratovolcano andesite	60.6	37	585	0.70473 ± 8	0.512626 ± 14
NT 23	stratovolcano andesite	61.1	66	427	0.70428 ± 7	
NT 24	stratovolcano andesite	62.1	74	454	0.70421	0.512731
NH 26	stratovolcano andesite	62.6	39	608	0.70488 ± 8	0.512567
NT 5	rhyolite	71.6	100	282	0.70511 ± 8	0.512496 ± 14
NH 33	rhyolite	73.9	192	7	0.70506 ± 4	0.512557 ± 17

+ Sample locations are as follows:

Alkali basalt: NT44 and NT48 from Actopan area (Fig. 3); U4 and U49 from Palma Sola area (Fig. 3).

Tholeiite: NT31 from Palma Sola area (Fig. 3).

Basalt: NH22 from Naolinco de Victoria area (Fig. 3); NT60 from Coatepec area (Fig. 2); NH12 from Saltillo area (Fig. 2); NH20 from Alto Lucero area (Fig. 3); NH3 from Ciudad Serdán - Orizaba area (Fig. 2); NT13 from La Gloria area (Fig. 2).

Basaltic andesite: NT57 from Acatlán area (Fig. 3); NT41 from Palma Sola area (Fig. 3); NH4 and NH5 from Ciudad Serdán - Orizaba area (Fig. 2); NT17 from Cerro Malpais area (Fig. 2); NT12 from Perote area (Fig. 2).

Monogenetic basaltic andesite: NT61 from Coatepec area (Fig. 2).

Monogenetic andesite: NT47 from south of Actopan (Fig. 3); NT54 and NT50 from Jalapa area (Fig. 3); NT18 from Ciudad Serdán area (Fig. 2); NT11 from Cerro Malpais area (Fig. 2); NT27 from Las Vigas area (Fig. 2).

Stratovolcano andesite: NT7 from Cerro Derrumbadas area (Fig. 2); NT23 and NT24 from Cofre de Perote area (Fig. 2); NH26 from Pico de Orizaba area (Fig. 2).

Rhyolite: NT5 from Cerro Derrumbadas area (Fig. 2); NH33 from Cerro Pinto area (Fig. 2).

Table 1 (Cont.)

According to the subdivision of the easternmost TMVB into geological units, proposed by Negendank *et al.* (1985), the samples are distributed as follows:

The Altiplano area (Oriental Basin):	NH12, NT13, NH4, NH5, NT17, NT12, NT18, NT11, NT7, NH5 and NH33 (approximately left half area, left of Pico de Orizaba, in Fig. 2).
Cofre de Perote - Pico de Orizaba range:	NT60, NH3, NT61, NT27, NT23, NT24 and NH26 (right half area in Fig. 2).
Jalapa - Naolinco area:	NT44, NT48, NH22, NH20, NT57, NT47, NT54 and NT50 (left half area in Fig. 3).
Palma Sola Massif:	U4, U49, NT31 and NT41 (right half area in Fig. 3).

* The classification is based on a K_2O - SiO_2 diagram (Negendank *et al.*, 1985; Peccerillo and Taylor, 1976).

** Measured by XRF (Cherry *et al.*, 1967, 1970); the total propagated analytical errors range as follows $SiO_2 = 0.5$ rel.%, Rb and Sr = 5 rel.%

+ The $^{87}Sr/^{86}Sr$ ratios are normalized to $^{86}Sr/^{88}Sr = 0.11940$ and adjusted to SRM 987 $^{87}Sr/^{86}Sr$ ratio of 0.71014. The measured ratio for the SRM standard was 0.71041 ± 0.00004 during the period of study. The errors for the Sr isotopic ratios are expressed as two standard deviations of the mean.

*** The $^{143}Nd/^{144}Nd$ ratios are normalized to $^{146}Nd/^{144}Nd = 0.72190$. The measured value for the La Jolla Standard was 0.511833 ± 0.000012 ($n = 82$) during the period of study.

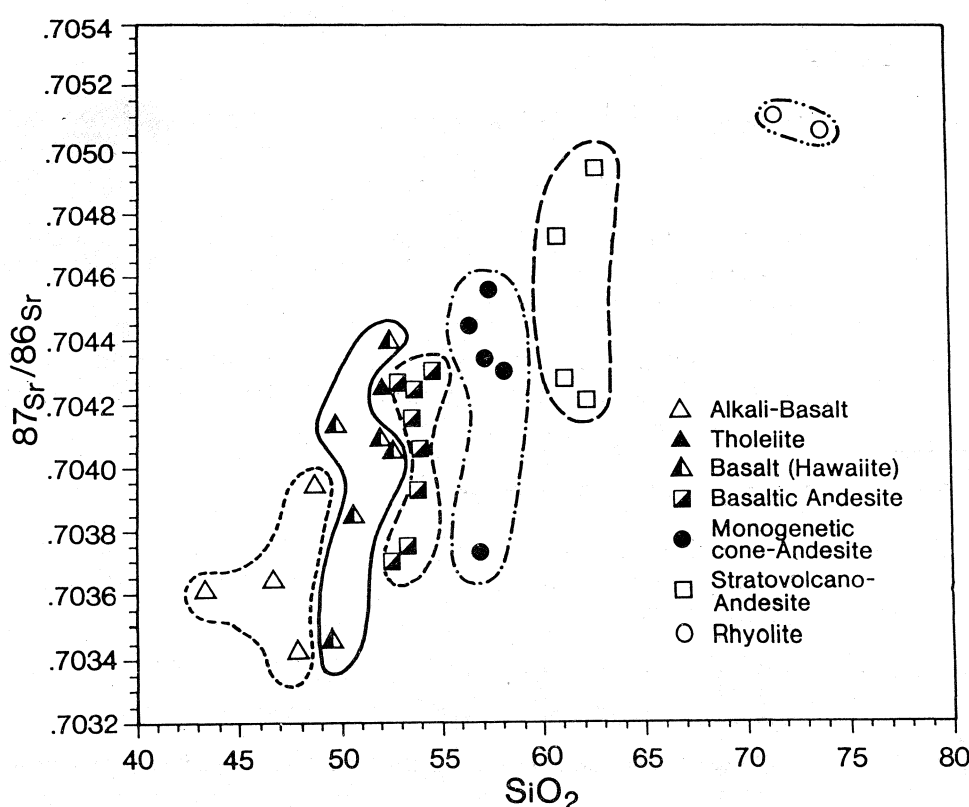
Fig. 5. $^{87}Sr/^{86}Sr$ versus SiO_2 for the volcanics of the eastern TMVB.

Table 2

Major, trace and REE element abundances (according to Negendank *et al.*, 1985) of selected samples from the eastern Trans-Mexican Volcanic Belt

	NH 33	NT 5	NT 1	NH 26	NT 24
SiO₂	73,9	71,6	63,1	62,6	62,1
TiO₂	0,03	0,15	0,72	0,66	0,92
Al₂O₃	14,0	15,7	17,1	18,1	16,6
Fe₂O₃	0,2	1,45	4,47	2,09	2,32
FeO	0,49	0,92	0,19	2,77	2,73
MnO	0,14	0,04	0,08	0,08	0,08
MgO	0,09	0,28	2,42	2,35	3,15
CaO	0,49	1,81	5,86	4,44	5,38
Na₂O	4,47	4,62	4,13	4,63	3,89
K₂O	4,09	3,44	1,3	1,89	2,68
P₂O₅	0,04	0,08	0,25	0,19	0,23
H₂O+	2,0	0,07	0,25	0,26	0,31
CO₂	0,03	0,08	0,24	0,15	0,05
Sum	99,97	100,24	100,11	100,21	100,44
Cr	4	4	15	14	44
Co	< 1	3	9	12	14
Ni	5	4	10	8	30
Cu	< 1	2	13	19	28
Zn	46	68	57	58	59
Rb	192	100	16	39	74
Sr	22	275	1125	598	454
Y	24	9	20	18	22
Zr	667	150	54	109	209
Nb	23	14	4	5	16
Ba	< 50	898	409	712	611
La		25	16	11	25
Ce	10	75	36	29	53
Pb	19	17	6	9	12
Th	7	10	2	1	12
La			19	16	
Ce			36	31	
Nd			18	18	
Sm			3,9	3,8	
Eu			1,2	1,1	
Tb			0,36	0,36	
Dy			2,9	2,2	
Yb			1,4	1,2	
Lu			0,23	0,2	
Sc			8	9	
Cs			0,7	1,1	
Hf			3,4	3,3	
Th			2	2,6	
U			0,4	1	
Ta			0,2	0,3	

Table 2 (Cont.)

	NT 23	NT 7	NT 27	NT 11	NT 50
SiO₂	61,1	60,6	58,1	57,2	57,1
TiO₂	1,09	0,85	1,03	1,13	1,08
Al₂O₃	16,4	18,1	16,5	16,6	17,0
Fe₂O₃	1,99	1,75	2,68	1,34	4,73
FeO	3,96	3,57	3,67	5,36	2,5
MnO	0,1	0,09	0,01	0,11	0,12
MgO	2,73	2,82	3,96	5,0	4,36
CaO	5,04	5,9	6,68	6,57	7,04
Na₂O	4,05	4,23	3,82	3,87	3,73
K₂O	2,57	1,65	2,4	1,76	1,8
P₂O₅	0,27	0,22	0,27	0,37	0,29
H₂O+	0,89	0,22	0,38	0,38	0,59
CO₂	0,05	0,04	0,26	0,15	0,05
Sum	100,24	100,04	99,76	99,84	100,39
Cr	26	24	86	119	86
Co	16	14	18	25	20
Ni	13	9	21	67	30
Cu	15	11	23	26	33
Zn	70	61	65	79	74
Rb	66	39	74	39	47
Sr	413	578	503	484	527
Y	25	21	25	25	48
Zr	222	139	207	190	185
Nb	13	4	13	12	8
Ba	685	507	598	548	526
La	17	7	20	16	43
Ce	53	30	67	48	76
Pb	11	9	12	6	9
	9	3	14	< 1	8
La		18			54
Ce		40			72
Nd		21			40
Sm		4,6			10,6
Eu		1,3			2,4
Tb		0,61			1
Dy		3,4			7,4
Yb		1,7			3,2
Lu		0,27			0,48
Sc		12			18
Cs		1,9			1,8
Hf		4,3			4,7
Th		3,5			6,1
U		1,2			1,8
Ta		0,35			0,6

Table 2 (Cont.)

	NT 18	NT 54	NT 47	NT 61	NH 5
SiO₂	56,9	56,3	54,4	53,9	53,7
TiO₂	0,95	1,06	2,16	1,55	0,97
Al₂O₃	15,8	16,5	15,9	17,8	15,7
Fe₂O₃	2,63	3,69	6,56	6,02	2,39
FeO	4,03	3,07	3,19	2,54	5,08
MnO	0,11	0,11	0,13	0,13	0,12
MgO	5,64	5,88	3,15	4,4	8,69
CaO	8,28	7,04	6,15	7,73	8,71
Na₂O	3,44	3,74	4,05	3,93	3,11
K₂O	1,77	1,53	2,94	1,56	1,14
P₂O₅	0,27	0,27	1,02	0,37	0,25
H₂O+	0,51	0,57	0,32	0,35	0,25
CO₂	0,05	0,04	0,07	0,08	0,05
Sum	100,38	99,80	100,04	100,36	100,16
Cr	102	161	24	29	318
Co	22	23	27	27	27
Ni	24	93	23	30	91
Cu	36	29	96	34	51
Zn	71	72	104	88	70
Rb	26	34	100	34	18
Sr	861	497	403	546	666
Y	22	21	54	28	23
Zr	92	156	538	200	93
Nb	4	13	31	15	5
Ba	464	459	778	437	287
La	13	16	38	22	10
Ce	40	50	110	54	34
Pb	8	8	21	8	5
Th	4	3	21	5	1
La	22				
Ce	40				
Nd	28				
Sm	5,8				
Eu	1,6				
Tb	0,7				
Dy	3,5				
Yb	1,8				
Lu	0,34				
Sc	23				
Cs	1,1				
Hf	4,4				
Th	5,5				
U	1,6				
Ta	0,22				

Table 2 (Cont.)

	NT 12	NT 17	NH 4	NT 41	NT 13
SiO₂	53,4	53,4	53,3	52,8	52,8
TiO₂	1,48	1,37	0,97	1,92	1,09
Al₂O₃	18,1	16,5	15,7	17,7	16,2
Fe₂O₃	1,58	1,5	2,55	6,41	1,48
FeO	6,68	6,5	4,99	2,72	5,94
MnO	0,13	0,13	0,12	0,16	0,13
MgO	4,66	7,13	9,01	2,88	8,58
CaO	8,24	7,77	8,81	6,64	8,45
Na₂O	3,69	3,67	3,03	4,64	3,1
K₂O	1,41	1,35	1,12	2,53	1,65
P₂O₅	0,33	0,36	0,25	0,77	0,40
H₂O+	0,33	0,44	0,37	0,54	0,33
CO₂	0,04	0,19	0,05	0,05	0,19
Sum	100,07	100,31	100,27	99,76	100,34
Cr	49	213	341	13	378
Co	27	29	28	24	29
Ni	29	105	105	7	163
Cu	34	35	31	25	55
Zn	83	81	74	87	73
Rb	31	27	18	74	35
Sr	488	515	673	847	595
Y	29	26	23	35	25
Zr	185	167	94	290	177
Nb	11	11	5	34	10
Ba	395	427	279	861	598
La	10	16	11	32	25
Ce	38	48	31	101	70
Pb	6	7	6	8	8
Th	4	3	2	9	9
La	22	21	20	62	31
Ce	48	41	40	95	60
Nd	24	18	21	40	24
Sm	5,5	4,5	4,7	8	5,9
Eu	1,6	1,4	1,4	2	1,5
Tb	0,78	0,8	0,68	2,3	0,6
Dy	4	4	3,3	0,92	3,5
Yb	2,3	1,8	1,8	6,1	1,7
Lu	0,37	0,28	0,28	2,6	0,27
Sc	21	19	26	0,4	22
Cs	0,7	0,9	1		1,5
Hf	4,9	3,9	3,3		4,3
Th	3,5	2,3	2,9		8
U	1	0,7	0,8		2,2
Ta	0,8	0,6	0,28		0,7

Table 2 (Cont.)

	NT 60	NH 22	NT 48	U 49	U 4	NT 44
SiO₂	49,80	49,60	48,70	47,90	46,70	43,50
TiO₂	1,89	1,60	1,85	2,21	2,39	1,50
Al₂O₃	16,40	16,60	17,20	17,10	15,40	13,60
Fe₂O₃	7,73	1,80	8,84	9,29	8,54	4,57
FeO	3,75	8,37	1,49	1,99	3,03	4,89
MnO	0,17	0,16	0,15	0,25	0,17	0,17
MgO	6,87	7,82	5,68	4,83	5,85	10,50
CaO	8,45	9,67	9,75	9,35	10,30	14,30
Na₂O	3,34	3,45	3,22	3,47	3,33	2,88
K₂O	0,93	0,71	1,66	1,45	1,27	0,57
P₂O₅	0,39	0,27	0,64	0,75	0,72	0,87
H₂O+	0,68	0,18	0,39	0,97	0,96	2,20
CO₂	0,04	0,08	0,07	0,05	0,58	0,10
Sum	100,44	100,31	99,64	99,61	99,24	99,65
Cr	229	255	110	100	244	303
Co	45	41	36	43	42	39
Ni	118	95	38	51	120	143
Cu	46	55	37	43	49	18
Zn	109	87	92	89	87	78
Rb	15	14	50	30	26	27
Sr	455	381	823	828	934	1071
Y	33	29	32	49	29	29
Zr	181	144	214	183	167	125
Nb	11	9	18	23	28	65
Ba	283	189	803	739	538	1045
La	11	5	23	46	26	49
Ce	34	25	68	109	80	141
Pb	4	2	7	4	4	8
Th	< 1	< 1	6	4	4	14
La	20		40			
Ce	41		71			
Nd	22		34			
Sm	5,7		9			
Eu	1,7		2,3			
Tb	1		0,9			
Dy	4,7		5,3			
Yb	2,3		2			
Lu	0,36		0,33			
Sc	23		23			
Cs	0,3		2,1			
Hf	4,2		6,3			
Th	1,6		5,5			
U	0,5		1,4			
Ta	0,7		1,2			

Table 2 (Cont.)

	NT 57	NH 3	NH 20	NT 31	NH 12
SiO₂	52,7	52,4	52,2	52,2	50,6
TiO₂	1,26	0,90	1,36	1,37	1,49
Al₂O₃	18,0	16,1	16,5	16,9	15,9
Fe₂O₃	5,57	2,90	3,58	3,75	3,16
FeO	2,55	5,02	4,01	4,47	6,13
MnO	0,13	0,13	0,14	0,14	0,15
MgO	5,74	8,94	6,03	5,33	8,38
CaO	8,58	8,96	7,8	9,56	9,2
Na₂O	3,73	3,39	3,41	3,60	3,41
K₂O	1,1	1,1	3,24	1,17	1,09
P₂O₅	0,34	0,20	0,58	0,33	0,35
H₂O+	0,50	0,29	0,77	0,37	0,13
CO₂	0,07	0,05	0,08	0,98	0,15
Sum	100,27	100,38	99,70	100,17	100,14
Cr	119	309	242	86	327
Co	26	32	24	26	34
Ni	63	142	102	44	128
Cu	33	56	46	35	47
Zn	82	74	85	82	76
Rb	18	18	96	21	21
Sr	584	521	906	593	500
Y	27	21	34	27	26
Zr	170	89	325	160	146
Nb	12	4	38	8	10
Ba	465	438	1384	444	302
La	12	9	48	13	10
Ce	49	29	126	43	37
Pb	6	7	12	4	4
Th	3	2	15	< 1	2
La				24	22
Ce				55	50
Nd				30	24
Sm				6	5,3
Eu				1,8	1,7
Tb				0,69	0,83
Dy				4,2	3,7
Yb				2,4	2,2
Lu				0,38	0,32
Sc					29
Cs					1
Hf					4,6
Th					2,8
U					1
Ta					0,8

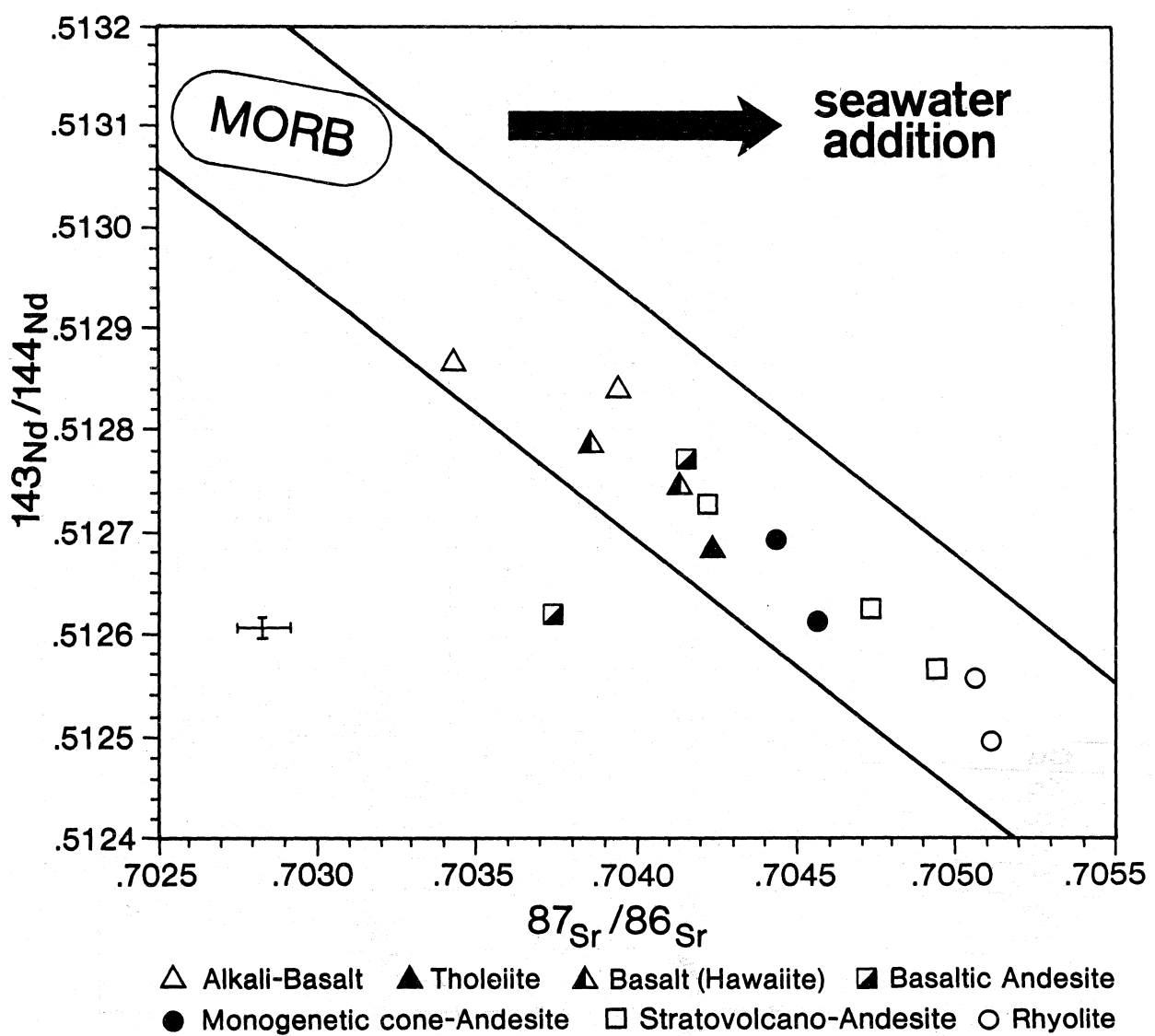


Fig. 6. $^{143}\text{Nd}/^{144}\text{Nd}$ versus $^{87}\text{Sr}/^{86}\text{Sr}$. The solid lines envelop the 'mantle array' (using the average values from Zindler *et al.*, 1982). TMVB data are plotted.

Table 3

Sr isotopic variation for the easternmost TMVB

alkali basalts	0.70342 - 0.70394 (n = 4)
basalts	0.70346 - 0.70439 (n = 6)
basaltic andesites	0.70370 - 0.70429 (n = 8)
monogenetic andesites	0.70374 - 0.70456 (n = 5)
stratovolcano andesites	0.70421 - 0.70488 (n = 5)
rhyolites	0.70506 - 0.70511 (n = 2)

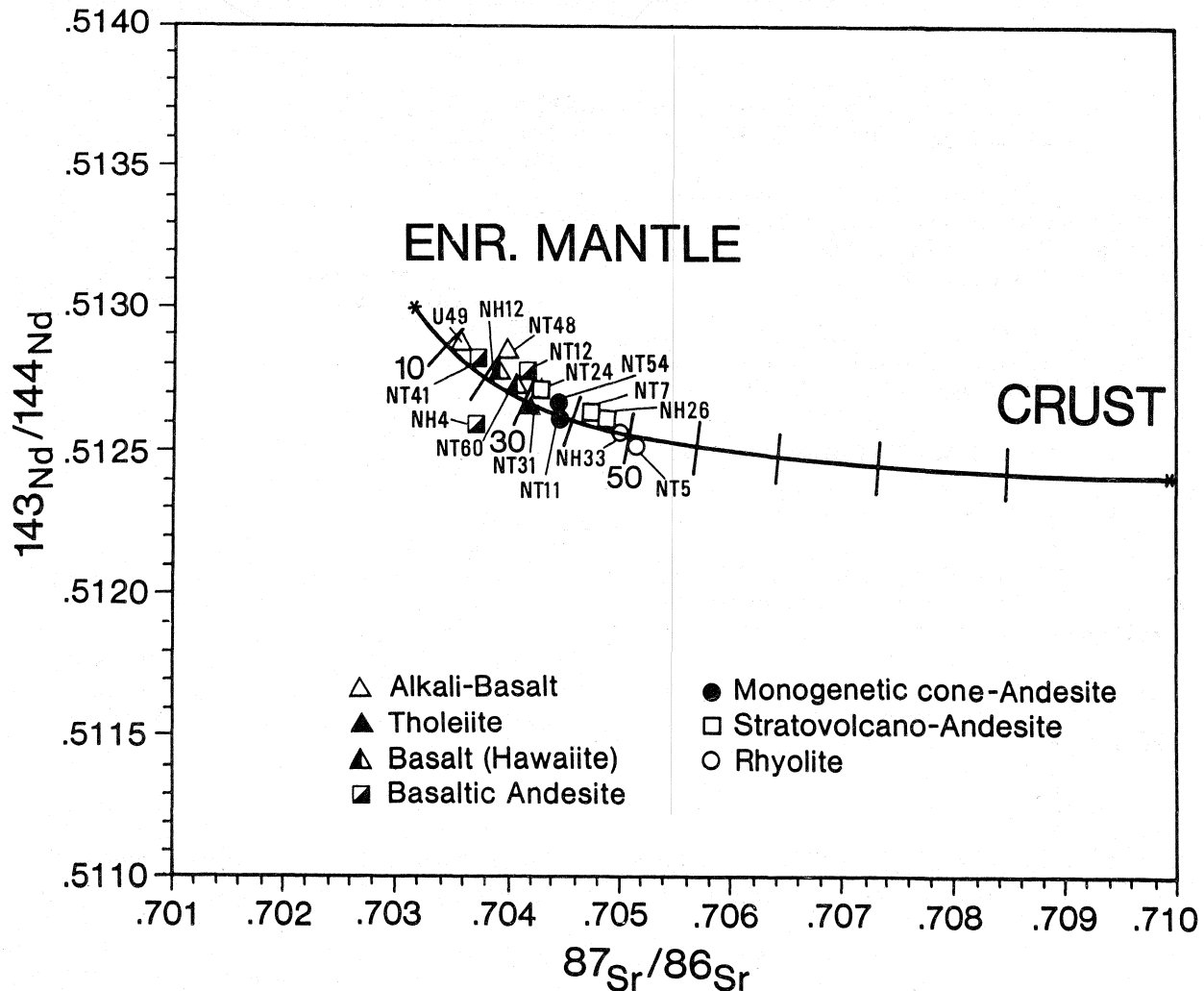


Fig. 7. Two component mixing model for the eastern TMVB, assuming $(\text{Sr}/\text{Nd})_{\text{EM}}/(\text{Sr}/\text{Nd})_{\text{CC}} = 3$ (EM = enriched mantle component; CC = crustal component). Estimates of the isotope ratios of the crustal end-member are based on S.P. VERMA's unpublished data.

ACKNOWLEDGEMENTS

We thank A.W. Hofmann for the use of experimental facilities at the Max-Planck-Institut für Chemie, Mainz and two anonymous reviewers for helpful comments on an earlier version of this paper. This work was supported by Deutsche Forschungsgemeinschaft (DFG) grant Tob. 53/12-1-2. S.P. Verma's visit to MPI was funded by Alexander von Humboldt foundation.

BIBLIOGRAPHY

- BESCH, Th., B. GRAUERT, H. J. TOBSCHALL and J. F. W. NEGENDANK, 1987. Evidence of assimilation during the genesis of subduction related volcanics in the eastern Trans Mexican Volcanic Belt. *Terra Cognita*, 7, 274-275.
- BESCH, Th., J.F.W. NEGENDANK, R. EMMERMANN and H. J. TOBSCHALL, 1988. Geochemical con-
- straints on the origin of calcalkaline and alkaline magmas of the eastern Trans-Mexican Volcanic Belt. *Geofís. Int.*, 27, 641-663.
- BRIQUEU, L., H. BOUGOULT and J. L. JORON, 1984. Quantification of Nb, Ta, Ti and V anomalies in magmas associated with subduction zones: petrogenetic implications. *Earth Planet. Sci. Lett.*, 68, 297-308.
- CANTAGREL, J.-M. and C. ROBIN, 1978. Géochimie isotopique du strontium dans quelques séries types du volcanisme de l'Est mexicain. *Bull. Soc. Geol. Fr.*, 20, 935-939.
- CHERRY, R. D., A. J. ERLANK and L. H. AHRENS, 1967. Observations on the Th/U relationship in zircons from granitic rocks and from kimberlites. *Geochim. Cosmochim. Acta*, 31, 2379-2387.
- CHERRY, R. D., J. B. M. HOBBS, A. J. ERLANK and J. P. WILLIS, 1970. Thorium, uranium, potassium,

- lead, strontium and rubidium in silicate rocks by Gamma-Spectroscopy and/or x-Ray Fluorescence. *Can. Spectrosc.*, 15, 3-9.
- DEMANT, A., 1978. Características del Eje Neovolcánico Transmexicano y sus problemas de interpretación. Univ. Nac. Autón. México, *Inst. Geol. Rev.*, 2, 172-187.
- DEMANT, A., 1981. L'axe néo-volcanique transmexicain: Etude volcanologique et pétrographique, Signification Géodynamique. Univ. de Droit, d'Economie et des Sciences d'Aix-Marseille. 259 p.
- DEPAOLO, D. J., 1981. Trace element and isotopic effects of combined wallrock assimilation and fractional crystallization. *Earth Planet. Sci. Lett.*, 53, 189-202.
- DEPAOLO, D. J. and G. J. WASSERBURG, 1979. Petrogenetic mixing models and Nd-Sr isotopic patterns. *Geochim. Cosmochim. Acta*, 43, 615-627.
- ELLAM, R. M. and C. J. HAWKESWORTH, 1987. LIL element and LILE/LREE ratios in island arc basalts: petrogenetic implications. *Terra Cognita*, 7, 415-416.
- HAWKESWORTH, C. J., R. K. O'NIONS, R. J. PANKHURST, P. J. HAMILTON and N. M. EVENSEN, 1977. A geochemical study of island-arc and backarc tholeiites from the Scotia Sea. *Earth Planet. Sci. Lett.*, 36, 253-262.
- HOLE, N. J., A. D. SAUNDERS, G. F. MARRINER and J. TARNEY, 1984. Subduction of pelagic sediments: implications for the origin of Ce-anomalous basalts from the Mariana Islands. *J. Geol. Soc. London*, 141, 453-472.
- JAGOUTZ, E., H. PALME, E. BADDENHAUSEN, K. BLUM, M. CENDALES, G. DREIBUS, B. SPETTEL, V. LORENZ and H. WÄNKE, 1979. The abundances of major, minor and trace elements in the earth's mantle as derived from primitive ultramafic nodules. Proc. 10th Lunar Planet. Sci. Conf., 2031-2050.
- KRAMM, U., A. B. BLAXLAND, V. A. KONOVOVA and B. GRAUERT, 1983. Origin of the Ilmenogorsk-Vishnevogorsk nepheline syenites, Urals, USSR, and their time of emplacement during the history of the Ural Fold Belt: a Rb-Sr study. *J. Geol.*, 91, 427-435.
- KUDO, A. M., M. E. JACKSON and J. W. HUSLER, 1985. Phase chemistry of recent andesite, dacite and rhyodacite of volcán Pico de Orizaba, Mexican Volcanic Belt: Evidence for xenolithic contamination. *Geofís. Int.*, 24, 679-689.
- MAHOOD, G. A. and A. N. HALLIDAY, 1987. Generation of high-silica rhyolite: a Nd, Sr, and O isotopic study of Sierra La Primavera, Mexican Neovolcanic Belt. *Contrib. Mineral. Petrol.*, 100, 183-191.
- MCBIRNEY, A. R., H. P. TAYLOR and R. L. ARMSTRONG, 1987. Paricutin re-examined: a classical example of crustal assimilation in calc-alkaline magma. *Contrib. Mineral. Petrol.*, 95, 4-20.
- MOORBATH, S., R. S. THORPE and J. L. GIBSON, 1978. Strontium isotope evidence for petrogenesis of Mexican andesites. *Nature*, 271, 437-438.
- NEGENDANK, J. F. W., R. EMMERMANN, R. KRAWCZYK, F. MOOSER, H. J. TOBSCHALL and D. WERLE, 1985. Geological and geochemical investigations on the eastern Trans Mexican Volcanic Belt. *Geofís. Int.*, 24, 477-575.
- NIXON, G. T., 1982. The relationship between Quaternary volcanism in central Mexico and the seismicity and structure of subducted ocean lithosphere. *Geol. Soc. Am. Bull.*, 93, 514-523.
- NIXON, G. T., A. DEMANT, R. L. ARMSTRONG and J. E. HARAKAL, 1987. K-Ar and geologic data bearing on the age and evolution of the Trans-Mexican Volcanic Belt. *Geofís. Int.*, 26, 109-158.
- PAL, S., M. LOPEZ-M., J. PEREZ-R. and D. J. TERRELL, 1978. Magma characterization in the Mexican Volcanic Belt (Mexico). *Bull. Volcanol.*, 41, 179-189.
- PEARCE, J. A., 1982. Trace element characteristics of lavas from destructive plate boundaries, In: R.S. Thorpe (Editor) Andesites: Orogenic Andesites and Related Rocks. John Wiley and Sons, 525-548.
- PECCERILLO, A. and S. R. TAYLOR, 1976. Geochemistry of Eocene calc-alkaline volcanic rocks from the Kastamonu area, Northern Turkey. *Contrib. Mineral. Petrol.*, 58, 63-81.
- PICHLER, H. and R. WEYL, 1976. Quaternary alkaline volcanic rocks in eastern Mexico and Central America. *Münster. Forsch. Geol. Paläont.*, 38/39, 179-200.
- ROBIN, C., 1976. Présence simultanée de magmatismes de significations tectoniques opposées dans l'est du Mexique. *Bull. Soc. Géol. Fr.*, 18, 1637-1645.
- ROBIN, C., 1982. Relations volcanologie-magmatologie-géodynamiques: Application au passage entre volcanismes alcalins et andésitiques dans le sud Mexicain (Axe Trans-mexicain et Province Alcaline Orientale). *Annal. Sci. l'Univ. Clermont-Ferrand II*, 30, 503 p.
- THORPE, R.S., 1977. Tectonic significance of alkaline volcanism in eastern Mexico. *Tectonophysics*, 40, 19-26.
- TOBSCHALL, H. J., R. EMMERMANN, A. W. HOFMANN and J. F. W. NEGENDANK, 1984. Zur Sr- und Nd-Isotopie von Andesiten des Ostteils des

- Transmexikanischen Vulkangürtels. 9. Geowiss. Lateinamerika Koll. Marburg, S. 167.
- VERMA, S. P., 1983. Magmagenesis and chamber processes at Los Humeros caldera, Mexico - Nd and Sr isotope data. *Nature*, 301, 52-55.
- VERMA, S. P., 1984. Alkali and alkaline earth element geochemistry of Los Humeros caldera, Puebla, Mexico. *J. Volcanol. Geotherm. Res.*, 20, 21-40.
- VERMA, S. P. (Editor), 1985. Special Volumes on Mexican Volcanic Belt, Parts 1 and 2. *Geofís. Int.*, 24-1 and 24-2.
- VERMA, S. P. (Editor), 1987a. Special Volumes on Mexican Volcanic Belt, Parts 3A and 3B. *Geofís. Int.*, 26-1 and 26-2.
- VERMA, S. P., 1987b. Mexican Volcanic Belt: Present state of knowledge and unsolved problems. *Geofís. Int.*, 26, 309-340.
- VERMA, S. P., 1994. Geochemical and isotopic constraints on the origin of mafic volcanism in central Mexico. *Miner. Mag.*, 58A, 938-939.
- VERMA, S. P. and M. A. ARMIENTA-H., 1985. $^{87}\text{Sr}/^{86}\text{Sr}$, alkali and alkaline earth element geochemistry of Chichinautzin Sierra, Mexico. *Geofís. Int.*, 24, 665-678.
- VERMA, S. P. and J. F. LUHR, 1993. Sr-Nd-Pb isotope and trace element geochemistry of calc-alkaline andesites from Volcán Colima, Mexico. *Geofís. Int.*, 32, 617-631.
- VERMA, S. P. and S. A. NELSON, 1989a. Isotopic and trace element constraints on the origin and evolution of alkaline and calc-alkaline magmas in the Northwestern Mexican Volcanic Belt. *J. Geophys. Res.*, 94, 4531-4533.
- VERMA, S. P. and S. A. NELSON, 1989b. Correction to: "Isotopic and trace element constraints on the origin and evolution of alkaline and calc-alkaline magmas in the Northwestern Mexican Volcanic Belt". *J. Geophys. Res.*, 94, 7679-7681.
- VERMA, S. P. and M. P. VERMA, 1986. A compilation of Sr and Nd isotope data on Mexico. *J. Geol. Soc. India*, 27, 130-143..
- VERMA, S. P., G. CARRASCO-NUÑEZ and M. MILAN, 1991. Geology and geochemistry of Amealco caldera, Qro., Mexico. In: S.P. VERMA (Editor) Calderas: Genesis, Structure and Unrest. *J. Volcanol. Geotherm. Res.*, 47, 105-127.
- VERMA, S. P., M. LOPEZ-MARTINEZ and D. J. TERRELL, 1985. Geochemistry of Tertiary igneous rocks from Arandas-Atotonilco area, Northeast Jalisco, Mexico. *Geofís. Int.*, 24, 31-45.
- WÄNKE, H., G. DREIBUS, and E. JAGOUTZ, 1984. Mantle chemistry and accretion of the Earth. In: A. Kröner, G.N. Hanson and A.M. Godwin (Editors) Archean Geochemistry. Springer, 1-24.
- WHITE, W. M. and A. W. HOFMANN, 1982. Sr and Nd isotope geochemistry of oceanic basalts and mantle evolution. *Nature*, 296, 821-825.
- WHITE, W. M. and J. PATCHETT, 1984. Hf-Nd-Sr isotopes and incompatible element abundances in island arcs: implications for magma origins and crust-mantle evolution. *Earth Planet. Sci. Lett.*, 67, 167-185.
- WHITFORD, D. J. and K. BLOOMFIELD, 1976. Geochemistry of Late Cenozoic volcanic rocks from Nevado de Toluca area, Mexico. *Carnegie Inst. Washington Yearb.*, 75, 207-213.
- WOOD, D. A., 1979. A variable veined suboceanic mantle: Genetic significance for mid-ocean ridge basalts from geochemical evidence. *Geology*, 7, 499-503.
- ZINDLER, A., E. JAGOUTZ and S. GOLDSTEIN, 1982. Nd, Sr and Pb isotopic systematics in a three-component mantle: a new perspective. *Nature*, 298, 519-523.
-
- Thomas Besch¹, Surendra P. Verma², Ulrich Kramm³, Jörg F.W. Negendank⁴, Heiner J. Tobischall⁵ and Rolf Emmermann⁶
- ¹ Lehreinheit Mineralogie, Institut für Geowissenschaften, Universität Mainz, 55122 Mainz, FRG.
- ² Max-Planck-Institut für Chemie, Abt. Geochemie, 55128 Mainz, FRG and Universität Trier, Abt. Geologie, 54296 Trier, FRG.; Present address: Laboratorio de Energía Solar, Instituto de Investigaciones en Materiales, UNAM, AP 34, Temixco, Mor. 62580, Mexico.
- ³ Universität Münster, Institut für Mineralogie, 48149 Münster, FRG.
- ⁴ Geoforschungszentrum Potsdam und Geowissenschaften, Universität Potsdam, 14473 Potsdam, FRG.
- ⁵ Institut für Geologie und Mineralogie, Universität Erlangen-Nürnberg, 91054 Erlangen, FRG.
- ⁶ Geoforschungszentrum Potsdam, 14473 Potsdam, FRG, and Institut für Geowissenschaften und Lithosphärenforschung, Universität Gießen, 35390 Gießen, FRG.

